Dynamic criticality far from equilibrium: One-loop flow of Burgers-Kardar-Parisi-Zhang systems with broken Galilean invariance

Philipp Strack

Dynamic criticality far-from-equilibrium: one-loop flow of Burgers-Kardar-Parisi-Zhang systems with broken Galilean invariance

Philipp Strack[*]

Institut für Theoretische Physik, Universität zu Köln, D-50937 Cologne, Germany and

Department of Physics, Harvard University, Cambridge MA 02138

(Dated: February 17, 2015)

Abstract

Burgers-Kardar-Parisi-Zhang (KPZ) scaling has recently (re-) surfaced in a variety of physical contexts, ranging from anharmonic chains to quantum systems such as open superfluids, in which a variety of random forces may be encountered and/or engineered. Motivated by these developments, we here provide a generalization of the KPZ universality class to situations with long-ranged temporal correlations in the noise, which purposefully break the Galilean invariance that is central to the conventional KPZ solution. We compute the phase diagram and critical exponents of the KPZ equation with $1/f$-noise ($\mathrm{KPZ}_{1/f}$) in spatial dimensions $1 \leq d < 4$ using the dynamic renormalization group with a frequency cutoff technique in a one-loop truncation. Distinct features of $\mathrm{KPZ}_{1/f}$ are: (i) a generically scale-invariant, rough phase at high noise levels that violates fluctuation-dissipation relations and exhibits hyperthermal statistics *even in d=1*, (ii) a fine-tuned roughening transition at which the flow fulfills an emergent thermal-like fluctuation-dissipation relation, that separates the rough phase from (iii) a *massive phase* in $1 < d < 4$ (in $d = 1$ the interface is always rough). We point out potential connections to nonlinear hydrodynamics with a reduced set of conservation laws and noisy quantum liquids.

---
[*]Electronic address: pstrack@physics.harvard.edu; URL: http://users.physics.harvard.edu/~pstrack

I. INTRODUCTION

A lot of effort across the physical sciences is currently being directed at the derivation of the laws of statistical mechanics far-from-(thermal)-equilibrium [1]. A prototypical question of interest begins with a many-particle system in a known initial state, whose statistics for example in energy space is known. Subsequently, the system is subjected to either a rapid change of its parameters or a non-equilibrium drive and/or dissipation. One then would like to understand how the statistical distributions evolve in time, in particular with regard to thermalization properties, that is, how quickly and by which mechanisms, energy/momenta are redistributed in phase space and real space. The steady-state distributions in the long-time limit $t \to \infty$ are also interesting.

Roughly speaking, there are two extreme scenarios: (i) Integrable systems with a large number of conservation laws whose thermalization is at least slow due to constraints in phase space from these conservation laws (see Ref. 2 and references therein). (ii) Granular or soft matter systems (such as hard spheres in a box), engineered liquids [3, 4], or randomly sputtered interfaces [5], in which the concept of temperature, a priori, does not make sense, there are typically fewer conserved quantities, and the dynamics is determined by geometric constraints, dimensionality, and/or the amount of disorder. Moreover, the amount of symmetry shapes the phase structure and associated transitions despite the absence of a well-defined free energy landscape far-from-equilibrium.

In order to broadly elucidate the role of conservation laws in prototypical far-from-equilibrium phase transitions, the present paper studies Burgers-Kardar-Parisi-Zhang systems after *explicitly breaking its key symmetry/conservation law: the Galilean invariance* of the randomly stirred Burgers fluid associated with seeing the same physics when looking at the fluid in a moving frame [6]. Another motivation is the possibility to learn about thermalization properties of quantum systems by finding ways to deform the "KPZ-attractive Lieb-Liniger bosons duality" [7–10] away from the integrable point/with less conservation laws.

In this paper, we perform a dynamic renormalization group analysis of the Burgers-Kardar-Parisi-Zhang equation subject to $1/f$-noise developing a frequency rescaling technique on the Keldysh contour.

A. Model: Cole-Hopf transformed KPZ$_{1/f}$ equation

Our calculations are based on the Cole-Hopf transformed KPZ equation (recapitulated below), when it becomes a gapless diffusion equation with multiplicative noise

$$\gamma \partial_t \phi = \nu_0 \nabla^2 \phi + \frac{\lambda}{2\nu_0} \phi \eta \tag{1}$$

with $\phi = \phi(t, \mathbf{x})$ a scalar field describing fluctuations in time and space around a growing average height level, γ a friction parameter, and ν_0 the viscosity in the Burgers fluid picture. The η-field acts as nonlinear, multiplicative noise [11] with coupling strength proportional to λ [12]. A simple way to break the Galilean invariance is to endow the noise with $1/f$-correlations in time such that in frequency representation

$$\overline{\eta(\omega', \mathbf{x}')\eta(\omega, \mathbf{x})} = D_{1/f}(\omega)\delta(\omega + \omega')\delta^{(d)}(\mathbf{x}' - \mathbf{x}) . \tag{2}$$

with ubiquitous $1/f$ or pink noise temporal correlations [13]

$$D_{1/f}(\omega) = \frac{1}{|\omega|} . \tag{3}$$

Several authors have considered temporally correlated noise in the context of KPZ [12, 14–16] and, more recently, the $O(N)$-model [17]. In particular, it was found that the conventional KPZ exponents may change as a consequence of correlations in the noise. However, within the dynamical renormalization group approach of Medina et al. [12], the interesting $1/f$-case could not be addressed due to the presence of infrared singularities also in the frequency integrations. It is one objective of the present paper to fill this gap.

Medina et al. [12] have mentioned impurities or charged ions at the interface as possibility to generate temporal long-ranged correlations in the noise. In the context of quantum systems, $1/f$ appears generically as charge noise in trapped ions for example [18, 19] and other types of noise can appear in the laser trapping potentials of ultra cold atoms [20].

B. Key results

From the solution of our renormalization group equations, we obtain Fig. 1 as the phase diagram from a one-loop flow of Eq. (1) with $1/f$-noise integrating fluctuations from large frequencies $\omega = \Lambda_0$ to the lowest frequencies $\omega = 0$. In spatial dimensionality $d = 2$, $d = 3$, a massive phase for small $\tilde{\lambda}_{\Lambda_0}$ transits into a rough or turbulent phase at a critical value $\tilde{\lambda}_{\Lambda_0,c}$.
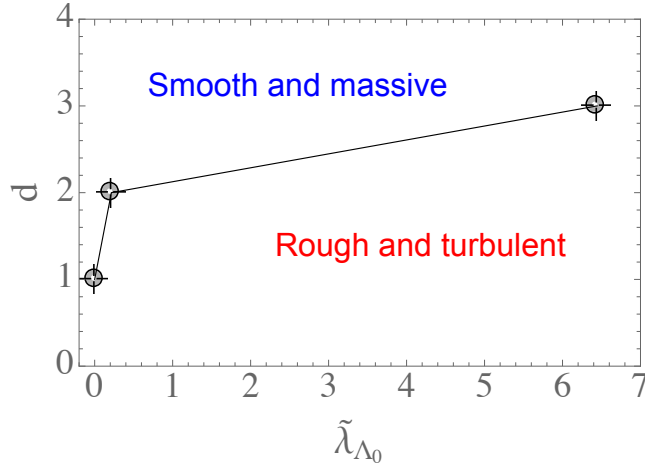
4

FIG. 1: Phase diagram of the KPZ equation with $1/f$ noise (computed points are connected as a guide to the eye) as a function of space dimensions (d) and strength of the bare noise vertex $\tilde{\lambda}_{\Lambda_0}$. The locators illustrate the roughening transition characterized by an unstable fixed point whose exponents fulfill an emergent thermal fluctuation-dissipation relation. In one dimension, the interface is always rough and any initial value of the noise vertex leads to the hyperthermal fixed point in the rough/turbulent phase. In contrast to conventional white noise KPZ phase diagram (e.g.: Ref. 21), here the fluctuation-dissipation theorem breaks down even in $d = 1$ and the smooth phase is manifestly massive.

The roughening transition and generically scale-invariant rough phase are distinguishable by different scaling forms of the response correlator:

$$\mathcal{R}(\omega, \mathbf{k}) = -2\mathrm{Im}\overline{\langle\phi(-\omega, -\mathbf{k})\phi(\omega, \mathbf{k})\rangle}_R \quad \Rightarrow \quad \mathcal{R}(s^z\omega, s\mathbf{k}) \propto \frac{1}{s^{2-\zeta_\gamma}}\mathcal{R} \tag{4}$$

and the independent Keldysh fluctuation correlator

$$C(\omega, \mathbf{k}) = i\,\overline{\langle\phi(-\omega, -\mathbf{k})\phi(\omega, \mathbf{k})\rangle}_K \quad \Rightarrow \quad C(s^z\omega, s\mathbf{k}) \propto \frac{1}{s^{4-2\zeta_\gamma+\zeta_{dK}}}C\,, \tag{5}$$

where the overbar denotes the average over the random forces or noise. ζ_γ is the anomalous exponent for the linear time derivative in Eq. (1) and appears in the effective viscosity $\tilde{\nu} = \frac{\nu_0}{\gamma}$. ζ_{dK} is the exponent for the effective noise spectrum, appearing in the statistical or Keldysh component defined below. A finite value of the exponent $\zeta_{\mathrm{hyper}} = \zeta_{dK} - \zeta_\gamma$ indicates deviations from thermal occupation of low-energy modes for which $\zeta_{\mathrm{hyper}} = 0$. This can be seen from the scaling form of the statistical distribution function

$$f(\omega, \mathbf{k}) = \frac{C(\omega, \mathbf{k})}{\mathcal{R}(\omega, \mathbf{k})} \quad \Rightarrow \quad f(s^z\omega, s\mathbf{k}) \Rightarrow \frac{1}{s^{2+(\zeta_{dK}-\zeta_\gamma)}}\frac{C}{\mathcal{R}}\,. \tag{6}$$
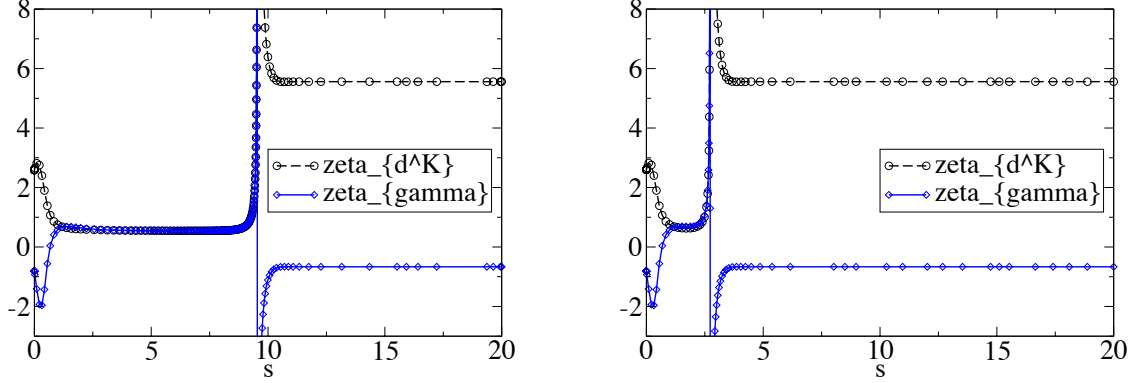
5

FIG. 2: Flow of the anomalous exponents slightly beyond the roughening transition in the rough phase in $d = 3$. The unstable fixed point plateau in which both exponents take the same value becomes progressively shorter the deeper one goes into the rough phase. The flow goes from the UV (left of plot) to IR (right of plot) via $\Lambda = \Lambda_0 \exp(-s)$. Left: $\tilde{\lambda}_{\Lambda_0} = 6.44294680824$, Right: $\tilde{\lambda}_{\Lambda_0} = 6.6443$, both larger than $\tilde{\lambda}_{\Lambda_0,c}$. The scaling plateaus of the roughening transition at which $\zeta_{d^K} = \zeta_\gamma = 0.54$ for $d = 3$ from Eq. (10) become unstable (at $s \approx 10$ in the left plot) and there is a steep transit into the rough phase, breaking the fluctuation-dissipation relation, at which $\zeta_{d^K} = 5.56$ and $\zeta_\gamma = -0.66$ from Table I in $d = 3$. Fine-tuned to 13 digits the critical noise vertex for the roughening transition is $\tilde{\lambda}_{\Lambda_0,c} = 6.4429468082319$ with $\Lambda_0 = 10$, $\Delta_{\Lambda_0} = \tilde{\Delta}_{\Lambda_0} = 0$ (no mass in the bare model Eq. (1)).

These exponents are measurable in an interface experiment via the roughness exponent

$$\chi_{\text{roughness}} = 1 - \frac{d}{2} + \frac{\zeta_{d^K} - \zeta_\gamma}{2} \tag{7}$$

which follows by comparison of Eq. (5) to the momentum representation of the height-height correlator $C_{hh}(\omega, \mathbf{q}) = \frac{1}{|\mathbf{q}|^{d+2\chi+z}} \tilde{C}(\omega/|\mathbf{q}|^z)$ [22] using further that in our case

$$z_{\text{dynamical}} = 2 - \zeta_\gamma . \tag{8}$$

For larger noise vertex $\tilde{\lambda}_{\Lambda_0} > \tilde{\lambda}_{\Lambda_0,c}$, in the rough or turbulent phase, the flow is attracted toward a gapless fixed point which breaks the fluctuation-dissipation relation of the KPZ equation with white noise [5, 22] as is shown in Fig. 2. In particular, for $d = 1$, the KPZ scaling relations $\chi + z = 2$ and $\chi = 1/2$ are violated. The low-energy statistics in this phase is "hyperthermal", that is the low-energy mode power-law divergence is stronger than thermal with $\zeta_{\text{hyper}} = 6.23$ in $d = 3$. Such infra-red enhanced population has been obtained at non-thermal fixed points of other,

6

	$d = 1$	d=2	d=3
$\chi_{\text{roughness}}$	11.34	5.15	2.61
$z_{\text{dynamical}}$	8	4	2.66
ζ_{d^K}	15.68	8.30	5.56
ζ_γ	−6	−2	−2/3
ζ_{hyper}	21.68	10.30	6.23

TABLE I: One-loop values of critical exponents in the generically scale-invariant, rough phase. Explicit violation of a thermal fluctuation-dissipation relation is observed for which instead $\zeta_\gamma = \zeta_{d^K}$ and $\zeta_{\text{hyper}} = 0$. The effective scale-dependent viscosity $\tilde{\nu}_\Lambda = \frac{\nu_0}{\gamma_\Lambda} \sim \Lambda^{\zeta_\gamma}$ diverges in entire the rough phase as $\zeta_\gamma < 0$. The fixed-point value of the nonlinear noise coupling goes to zero as $\epsilon = 4 - d \to 0$ leading to vanishing ζ_{d^K}, ζ_γ and $z_{\text{dynamical}} = 2$ in $d = 4$. Within our one-loop RG, ϵ may be regarded as the small parameter effectively controlling the flow; extrapolations to $d = 1, 2$ should be regarded as qualitative estimates only.

typically more complicated, field-theoretical models (see e.g. Refs. 23, 24 and references therein). The response function exponent turns out to be negative in the rough phase

$$\zeta_\gamma = \frac{2(d - 4)}{d} \tag{9}$$

and the full set of critical exponents in the rough phase are in Table I. The large value of the exponents in $d = 1$, $d = 2$ are due to the one-loop approximation and the fact the the noise vertex is relevant for $d < 4$. The one-loop computation is perturbatively controlled only close to $d = 4$.

The rough/turbulent phase is generically scale-invariant (sometimes also referred to as self-organized critical) in the sense that it is does not require fine-tuning of the coupling constants to reach it beyond a certain threshold [25, 26]. Rather, the *same* fixed point is reached for all $\tilde{\lambda}_{\Lambda_0} > \tilde{\lambda}_{\Lambda_0,c}$ as can be seen from flows of the mass parameter in Fig. 3. Note that the initial value of the mass Δ_{Λ_0} is always zero as appropriate for the gapless interface. Eq. (1) yields generic scale invariance with a relatively simple coupling to noise with a ubiquitous $1/f$-spectrum [13]. A
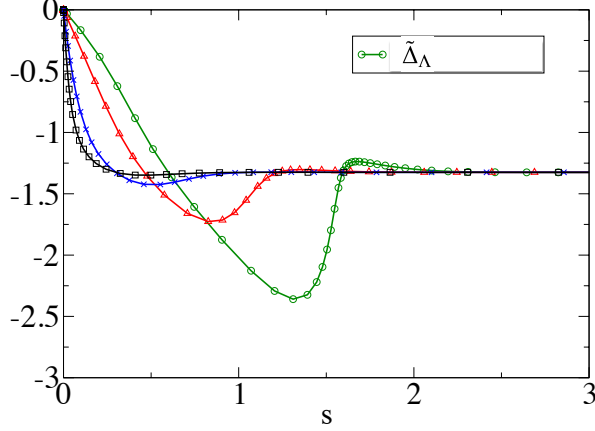
7

FIG. 3: Generically scale-invariant flows of the rescaled mass $\tilde{\Delta}_\Lambda$ in the rough phase in $d = 3$, which is attracted to the *same* fixed point value for different values of the noise vertex. $\tilde{\lambda}_{\Lambda_0} = 7, 10, 20, 30$ from green circles (7) to black squares (30). The initially zero mass (no mass in bare model Eq. (1)) is generated. The physical mass $\Delta_\Lambda = \tilde{\Delta}_\Lambda \Lambda^2 \gamma$ vanishes at the end of the flow for all couplings $\tilde{\lambda}_{\Lambda_0} \geq \tilde{\lambda}_{\Lambda_0,c}$. No fine-tuning of parameters required to reach this generically scale-invariant phase. The flow goes from the UV (left of plot) to IR (right of plot) via $\Lambda = \Lambda_0 \exp(-s)$.

further appealing feature of the simple model Eq. (1) with $1/f$-noise is that the rough phase can be penetrated with the relatively simple one-loop RG.

At the roughening transition (rt) in $d = 2$ and $d = 3$, the asymptotically gapless dynamics fulfills an emergent thermal-like fluctuation-dissipation relation ($\zeta_{\text{hyper}}^{\text{rt}} = 0$) with

$$\zeta_\gamma^{\text{rt}} = \zeta_{d^K}^{\text{rt}} = \frac{2d}{8+d} \quad \Rightarrow \quad z^{\text{rt}} = 2 - \zeta_\gamma^{\text{rt}} = \frac{16}{8+d} \tag{10}$$

where z^{rt} is the dynamical exponent at one-loop. Consequently, the roughness exponent

$$\chi_{\text{roughness}}^{\text{rt}} = 1 - \frac{d}{2} \tag{11}$$

becomes negative for $d > 2$. In the massive phase, scaling stops completely and none of the above exponents are defined. The roughening transition scaling is also seen in the unstable scaling plateaus of Fig. 2 and further numerical flows are presented in the main text, Subsec. IV C. At the roughening transition, the effective viscosity $\tilde{\nu}_\Lambda = \frac{\nu_0}{\gamma_\Lambda} \sim \Lambda^{\zeta_\gamma}$ vanishes as $\zeta_\gamma^{\text{rt}} > 0$ at one-loop. This is in contrast to the rough phase where the effective viscosity diverges as $\zeta_\gamma < 0$ from Table I.

8

C. Organization of paper

In Sec. II, we recapitulate the relations between the Burgers, KPZ, and diffusion equation with multiplicative noise. Following Medina, Hwa, Kardar, and Zhang (MHKZ) [12], we show how temporal correlations in the noise break the Galilean invariance of the Burgers fluid. Then, we elevate the equation to an action on the closed-time Keldysh action in Subsec. II B. In Subsec. II C, we briefly survey simplifications arising from the Galilean invariance such as exponent identities and a fluctuation-dissipation relation.

In Sec. III, we present the dynamic RG framework, explain the frequency cutoff technique and derive the form of the flow equations to one-loop order.

In Sec. IV, we present analytical and numerical solutions to the flow equations.

In Sec. V, we offer some conclusions, point toward physical systems where our results may become relevant for, and outline potential directions for future work.

II. BURGERS-KARDAR-PARISI-ZHANG EQUATION WITH $1/f$-NOISE

According to Kardar, Parisi, and Zhang [5], coarse-grained fluctuations in the growth of a d-dimensional interface subject to random depositions can be described in terms a of scalar height function

$$\gamma \frac{\partial h}{\partial t} = \nu_0 \nabla^2 h + \frac{\lambda}{2} (\nabla h)^2 + \eta \, , \tag{12}$$

where both the height $h = h(t, \mathbf{x})$ and the noise $\eta = \eta(t, \mathbf{x})$ are functions of time t and d-dimensional interface space spanned by $\mathbf{x}$.

Upon identifying the height with a vorticity-free velocity field $\mathbf{v} = -\nabla h$ and the random deposition noise with a random stirring force $\mathbf{f} = -\nabla \eta$, Eq. (12) is equivalent to the Burgers equation

$$\gamma \partial_t \mathbf{v} + \lambda \mathbf{v} \cdot \nabla \mathbf{v} = \nu_0 \nabla^2 \mathbf{v} + \mathbf{f} \, , \tag{13}$$

where ν_0 is the fluid viscosity, and the coefficient λ parametrizes the relative strength of the nonlinear, convective term [27]. In this paper, we will work with the representation of Eq. (12) as a diffusion equation for $\phi(t, \mathbf{x}) = \exp\left[\frac{\lambda}{2\nu_0\gamma} h(t, \mathbf{x})\right]$ [28] given above in Eq. (1). Under the Cole-Hopf transform the scaling behavior of the correlators for the physical height variable h and ϕ are proportional to each other

$$C_{hh} = \langle h(\mathbf{x}, t) h(\mathbf{x}', t') \rangle = \frac{4\nu_0^2 \gamma^2}{\lambda^2} \langle \ln \phi(\mathbf{x}, t) \ln \phi(\mathbf{x}', t') \rangle \sim \frac{4\nu_0^2 \gamma^2}{\lambda^2} C_{\phi\phi} \, . \tag{14}$$

9

A. Broken Galilean invariance from $1/f$-noise

The form of the noise correlator $\overline{\eta(t', \mathbf{x}')\eta(t, \mathbf{x})}$ in Eq. (3) determines the physical context and shapes the solution space of Eqs. (1,12,13). Temporal correlations in the noise break the Galilean invariance of the Burgers equation (13) under

$$\mathbf{v}(t, \mathbf{x}) \to \mathbf{v}_0 + \mathbf{v}'(\mathbf{x} - \lambda \mathbf{v}_0 t, t) \tag{15}$$

associated with looking at the fluid in a moving frame [6, 12]. To be self-contained, we now recapitulate why this is so following App. B of Ref. 12. For the interface equation (12) the Galilean invariance translates into invariance under infinitesimal tilts by a small angle ϵ

$$h' = h + \boldsymbol{\epsilon} \cdot \mathbf{x}$$

$$\mathbf{x}' = \mathbf{x} + \lambda \boldsymbol{\epsilon} t'$$

$$t' = t \tag{16}$$

It is easy to see that the deterministic part of Eq. (12) is invariant under Eq. (16). It is also invariant under constant height shifts $h \to h + \text{const}$ due to the absence of mass term or pinning potential. The transformed equation for h' is subject to transformed noise $\eta'(t', \mathbf{x}') = \eta(t', \mathbf{x} + \lambda \boldsymbol{\epsilon} t')$ implying for the noise correlator

$$
\begin{aligned}
F' = \overline{\eta'(t_1', \mathbf{x}_1')\eta'(t_2', \mathbf{x}_2')} &= \overline{\eta(t_1, \mathbf{x}_1 + \lambda \boldsymbol{\epsilon} t_1)\eta(t_2, \mathbf{x}_2 + \lambda \boldsymbol{\epsilon} t_2)} \\
&= F(t_1 - t_2, \mathbf{x}_1 - \mathbf{x}_2 + \lambda \boldsymbol{\epsilon}(t_1 - t_2)) \\
&= \delta(t_1 - t_2)F(\mathbf{x}_1 - \mathbf{x}_2 + \lambda \boldsymbol{\epsilon}(t_1 - t_2)) = \delta(t_1 - t_2)F(\mathbf{x}_1 - \mathbf{x}_2) = F \quad (17)
\end{aligned}
$$

where the last line is only true if the noise has no correlations in time i. e. $F(t, \mathbf{x}) = \delta(t)F(\mathbf{x})$. Our choice Eq. (3) corresponds to power-law correlations in real time and violates the invariance Eq. (17), as announced in the Introduction.

B. Keldysh path integral representation

In order to explore the large distance and long time physics of the Burgers-Kardar-Parisi-Zhang systems subject to $1/f$-noise, we elevate the stochastic differential equation problem Eq. (1) plus Eq. (3) to a Keldysh path integral [28, 29] on the closed time contour [55]. Wherever possible, we

10

will follow the notation of Frey and Täuber [22], who reviewed and performed this procedure and have given Ward and exponent identities for the related Janssen-De Dominicis functional.

The random forces are taken to be Gaussian-distributed

$$W[\eta] \propto \exp\left\{ -\int d^d x \int d\omega \frac{1}{2} \eta(\omega, \mathbf{x}) |\omega| \eta(\omega, \mathbf{x}) \right\} . \tag{18}$$

Then, the fluctuations in η can be included on the same footing as the fluctuations of ϕ in the Keldysh generating functional

$$Z = \int \mathcal{D}\eta W[\eta] \mathcal{D}(\phi, \tilde{\phi}) e^{i(S_\phi[\phi,\tilde{\phi}] - \int_{t,\mathbf{x}} \eta\phi\tilde{\phi})}$$

$$\equiv \int \mathcal{D}(\eta, \phi, \tilde{\phi}) e^{i(S_\phi[\phi,\tilde{\phi}] + S_\eta[\eta] + S_\lambda[\phi,\tilde{\phi},\eta])} . \tag{19}$$

The momentum-independent noise propagator is now complex-valued

$$S_\eta[\eta] = \frac{1}{2} \int_{\omega,\mathbf{q}} \eta(-\omega, -\mathbf{q}) \left[G^\eta(\omega) \right]^{-1} \eta(\omega, \mathbf{q}). \tag{20}$$

with

$$G^\eta(\omega) = \frac{-i}{|\omega|} . \tag{21}$$

Note that the momentum integrations here is bounded in the UV by some short-distance cutoff by virtue of a necessary smallest physical distance below which the noise is spatially uncorrelated and the continuum description must be replaced by a discrete theory of lattice sites/grains.

The multiplicative noise term in Eq. (1) results in a trilinear noise vertex

$$S_\lambda[\phi, \tilde{\phi}, \eta] = -\int_t dt \int d^d x \frac{\lambda}{2\nu_0} \eta(t, \mathbf{x}) \tilde{\phi}(t, \mathbf{x}) \phi(t, \mathbf{x}) \tag{22}$$

Finally, the dynamics, diffusion, and statistics (Keldysh $\tilde{\phi}\tilde{\phi}$-component) of the ϕ-fields are comprised in a matrix propagator

$$S_\phi[\phi, \tilde{\phi}] = \frac{1}{2} \int d\omega \int d^d k \left(\phi \; \tilde{\phi} \right) \begin{pmatrix} 0 & \left[G^A(\omega, \mathbf{k}) \right]^{-1} \\ \left[G^R(\omega, \mathbf{k}) \right]^{-1} & D^K \end{pmatrix} \begin{pmatrix} \phi \\ \tilde{\phi} \end{pmatrix} \tag{23}$$

with the bare retarded and advanced Greens function given by

$$G^R(\omega, \mathbf{k}) = \frac{1}{i\gamma\omega - \nu_0 \mathbf{k}^2} ,$$

$$G^A(\omega, \mathbf{k}) = \frac{1}{-i\gamma\omega - \nu_0 \mathbf{k}^2} , \tag{24}$$

11

The statistical Keldysh component D^K contains the effective noise spectrum and will later be determined by loop corrections. Note that in absence of the initially zero D^K, the *bare* action Eq. (22) consists only of power of $\tilde{\phi}\phi$, which can also be traced to a kind of gauge transformation related to Galilean invariance [30]. The bare action still describes a gapless interface and is invariant under constant shifts of $\phi \to \phi + \text{const}$. As we discussed, without Galilean invariance, the action is not protected against mass generation and we will allow for such terms to be generated in the renormalization group (RG) flow below in Sec. III.

C. Mini-recap of known results without broken Galilean invariance

We here briefly recollect some previous results of the Burgers-KPZ field theories focussing in particular on the simplifications due to Galilean invariance in the case of temporally white noise. In spatial dimension $d < 2$ KPZ interfaces are always rough for any value of the nonlinearity λ, see e.g.: Ref. 21. For $d > 2$, a smooth phase is stable for small λ and there is a line of non-equilibrium roughening transitions separating the two. An important consequence of the ability to phrase the KPZ problem in one dimension as an "equilibrium" partition function of an elastic string in a random potential [5, 31] are fluctuation-dissipation relations [32] and Ward identities [22]. In particular, these insure that (i) the noise vertex λ is not renormalized at all orders in perturbation theory, (ii) the fluctuation spectrum D scales similarly to the dissipative viscosity $D/\nu_0 \to \text{const}$, and (iii) that the roughness exponent χ and dynamical exponent z fulfill the exact relation $\chi + z = 2$ with $z = 3/2$ [5, 12]. In absence of Galilean invariance, (i) - (iii) do not hold anymore. In particular also the continuous shift invariance $h \to h + \text{const}$ can now be violated by loop corrections.

To explore the interface dynamics constrained by only a reduced set conserved quantities (essentially only momentum and parity), we next perform a dynamic renormalization group analysis.

III. DYNAMIC RENORMALIZATION GROUP

We will compute the one-loop RG flow of the action Eq. (19) employing a frequency cutoff, that is, rescaling frequencies and integrating over all momenta at each RG step. Our analysis will be framed in the context of the flow equation for the effective Keldysh action $\Gamma_\Lambda[\phi, \eta]$ as a function of a continuous flow parameter Λ (see Refs. 33, 34 for condensed matter applications):

$$\partial_\Lambda \Gamma_\Lambda[\phi, \eta] = \frac{i}{2} \text{Tr} \left[\frac{\dot{\mathcal{R}}}{\Gamma_\Lambda^{(2)}[\phi, \eta] + \mathcal{R}} \right], \tag{25}$$

where the trace stands for a frequency and momentum integration and a simple matrix trace in field space over the c and q components, and the noise field η, respectively. $\mathcal{R}$ is a matrix containing cutoff functions (specified below) as convenient for the field basis (ϕ_c, ϕ_q, η):

$$\mathcal{R} = \begin{pmatrix} 0 & R_\Lambda^\phi & 0 \\ R_\Lambda^\phi & 0 & 0 \\ 0 & 0 & R_\Lambda^\eta \end{pmatrix}$$

$\Gamma^{(2)}$ is a matrix containing the second field derivatives of Γ evaluated at zero field whose inverse contains the scale-dependent Green's functions that we define below.

Before proceeding, let us mention previous works that employed the flow equation for the effective action, Eq. (25), for the KPZ problem with white [35–37] and spatially correlated noise [38]. These works highlighted the importance of the frequency and momentum dependence of the running couplings, especially to obtain quantitative estimates of critical exponents. We will see below to capture the qualitative flow for $1/f$ noise correlations, a one-loop truncation is sufficient. Once overcome the difficulty of rescaling frequencies, the dynamical RG for the $1/f$ case is actually *simpler* than for the white noise case where no propagator renormalization occur to any order in the loop expansion [28].

A. Truncation of the effective action

We now specify which parameters we keep out of the formally large set of coupling constants that can be generated under the RG flow. In particular, it will be important to introduce independent parameters for the response function and the Keldysh spectrum. That allows the flow to break equilibrium-like fluctuation-dissipation relations. We also introduce a mass term. Note that ϕ, $\tilde{\phi}$
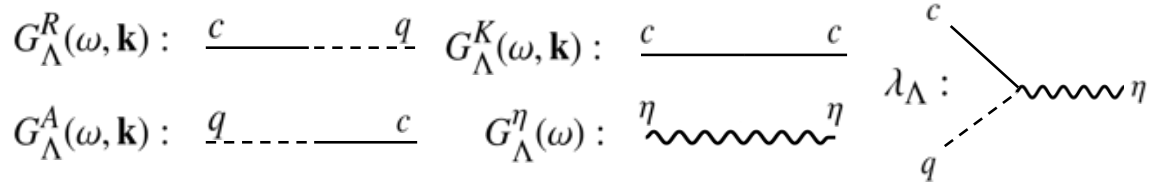
FIG. 4: Propagators and vertices appearing in the Keldysh action.

and η all have bare scaling dimension $\left[\frac{d}{2}\right]$ under bare $\omega \sim \Lambda^2$ power counting. As discussed in the Introduction, this makes the trilinear noise vertex λ_Λ formally relevant in $d < 4$.

Propagator renormalizations are captured by introducing four flowing parameters γ_Λ, A_Λ, a mass term Δ_Λ, and d_Λ^K for the (independent) Keldysh component. Together with the noise vertex, this is also the minimal set of couplings that one would have to renormalize for example within a field-theoretic RG analysis [22]. Including the additive, scale-dependent cutoff function R_Λ into Eq. (23) the quadratic part of the flowing action is

$$\Gamma_\Lambda^{(2)\phi} = \frac{1}{2} \int_k \left(\phi \, \tilde{\phi} \right) \begin{pmatrix} 0 & \left[G_\Lambda^A(\omega, \mathbf{k}) \right]^{-1} \\ \left[G_\Lambda^R(\omega, \mathbf{k}) \right]^{-1} & D_\Lambda^K(\omega) \end{pmatrix} \begin{pmatrix} \phi \\ \tilde{\phi} \end{pmatrix} \tag{26}$$

with the now scale-dependent, retarded and advanced propagators

$$G_\Lambda^R(\omega, \mathbf{k}) = \frac{1}{i\gamma_\Lambda \omega - (A_\Lambda \mathbf{k}^2 + \Delta_\Lambda) + R_\Lambda^R(\omega)} \, ,$$

$$G_\Lambda^A(\omega, \mathbf{k}) = \frac{1}{-i\gamma_\Lambda \omega - (A_\Lambda \mathbf{k}^2 + \Delta_\Lambda) + R_\Lambda^A(\omega)} \, , \tag{27}$$

where the frequency cutoffs are complex conjugates of one another $R_\Lambda^A(\omega) = \left[R_\Lambda^R(\omega) \right]^*$ and defined below. In contrast to the problem with full Galilean invariance, we will see that here a mass term (as well as nontrivial propagator renormalization via γ_Λ discussed further below) are generated at one loop – we capture this flow by introducing Δ_Λ.

The Keldysh propagator $G^K = -G^R D^K G^A$ with $D_\Lambda^K(\omega) = 2id_\Lambda^K$ is

$$G_\Lambda^K(\omega, \mathbf{k}) = \frac{-2id_\Lambda^K}{\left| i\gamma_\Lambda \omega - (A_\Lambda \mathbf{k}^2 + \Delta_\Lambda) + R_\Lambda^R(\omega) \right|^2} \, . \tag{28}$$

At one-loop, the momentum coefficient does not flow and it remains fixed at its initial value $A_\Lambda = \nu_0$ from Eq. (1).

The flowing trilinear noise vertex

$$\Gamma_\Lambda^{(3)} = -\int_{t,\mathbf{x}} \lambda_\Lambda \eta \tilde{\phi} \phi \tag{29}$$

14

is related to the bare vertex Eq. (22) at the beginning of the flow via $\lambda_{\Lambda=\Lambda_0} = \frac{\lambda}{2\nu_0}$.

The quadratic noise part in the action

$$\Gamma_\Lambda^{(2)\eta} = \frac{1}{2} \int_k \eta \left[G_\Lambda^\eta(\omega) \right]^{-1} \eta \tag{30}$$

is not renormalized and the inverse propagator needs only be supplemented by the cutoff (also defined below)

$$G_\Lambda^\eta(\omega) = \frac{-i}{|\omega| + R_\Lambda^\eta(\omega)} . \tag{31}$$

By endowing the noise propagator with a cutoff, the noise average is performed continuously along Λ, which may be viewed as flowing from the short time dynamics at large Λ to the long time dynamics at $\Lambda \to 0$. The Feynman graph elements of the flowing action are shown in Fig. 4.

B. Frequency cutoff technique

As announced above, we will use frequency regulators with Eq. (25), which in Wilsonian RG language corresponds to rescaling frequencies and integrating over all momenta at each RG step.

The specific form of the frequency regulator for the noise field is

$$R_\Lambda^\eta(\omega) = \left(-|\omega| + \Lambda^2 \right) \theta \left[\Lambda^2 - |\omega| \right]$$
$$\partial_\Lambda R_\Lambda^\eta(\omega) = 2\Lambda \theta \left(\Lambda^2 - |\omega| \right) , \tag{32}$$

and for the ϕ-field we have

$$R_\Lambda^R(\omega) = \gamma \left(-i\omega + i\mathrm{sgn}(\omega)\Lambda^2 \right) \theta \left[\Lambda^2 - |\omega| \right]$$
$$\dot{R}_\Lambda^R(\omega) \equiv \partial_\Lambda R_\Lambda^R(\omega) = 2\Lambda i\gamma \mathrm{sgn}(\omega)\theta \left[\Lambda^2 - |\omega| \right] \tag{33}$$

and for its advanced complex conjugate

$$R_\Lambda^A(\omega) = \gamma \left(+i\omega - i\mathrm{sgn}(\omega)\Lambda^2 \right) \theta \left[\Lambda^2 - |\omega| \right]$$
$$\dot{R}_\Lambda^A(\omega) \equiv \partial_\Lambda R_\Lambda^A(\omega) = -2\Lambda i\gamma \mathrm{sgn}(\omega)\theta \left[\Lambda^2 - |\omega| \right] . \tag{34}$$

We also dropped, as usual, the higher-order scale derivatives $\partial_\Lambda \gamma$ in these expressions. Hard (e.g.[39]) and soft (e.g. [40]) frequency cutoffs are frequently also being applied in RG studies of strongly correlated fermionic systems.

It is well known that frequency regulators breaks the analyticity of propagators in the complex plane. In particular, unphysical contributions could be generated from loop integrations that would/should actually vanish: integrals with all poles in one half-plane, for example $\int d\omega \left(G^{R/A}(\omega)\right)^n$, which are identically zero upon closing the contour in the "other" half plane, would give a finite contribution with a frequency cutoff. In our flow equations below, such graphs do not appear at the one-loop level. Instead, we only encounter products of the noise propagator with the retarded and advanced propagators $\sim \int d\omega G^\eta(\omega) G^{R/A}(\omega)$, which give finite, and similar, contributions with or without frequency cutoffs [56].

Note that, as we discuss below, we also get around performing the frequency derivative of the cutoff to extract the flow of γ by using an exponent identity that equates the flow of γ with that of the noise vertex λ.

With this cutoff choice, the frequency integrations over the one-loop contractions (below in Eq. (38)) become simple due the cutoff choice and for the rotationally symmetric momentum integrations it is convenient to use a rescaled momentum variable $\tilde{\mathbf{k}}^2 = \frac{A}{\gamma} \frac{\mathbf{k}^2}{\Lambda^2}$ such that the momentum integration measure becomes

$$d^d\mathbf{k} \rightarrow d^d\tilde{\mathbf{k}} \, \Lambda^d \left(\frac{\gamma}{A}\right)^{d/2} . \tag{35}$$

As announced above, we expect the continuum description to be valid only up to a short-distance of UV-momentum cutoff, below which the the granular/lattice structure of the interface becomes important. In order to regulate physically unimportant UV-divergences in the momentum integrations we systematically include only "on-shell" and smaller momenta into the flow

$$\mathbf{k}^2 \leq \frac{\gamma}{A}\Lambda^2 , \quad \tilde{\mathbf{k}}^2 \leq 1 . \tag{36}$$

As $\Lambda \rightarrow 0$, this is a shrinking ball around the origin in momentum space, whose volume is continuously adapted as γ flows, too. This mimicks the UV behavior from a Litim-type cutoff in momentum space, which regulates both, IR and UV divergences [41]. We have checked that the findings and fixed points reported below do not qualitatively seem to depend on the regularization procedure and choice of cutoffs. We have repeated the calculation for a different cutoff and different UV regularization procedure and found similar results [57]
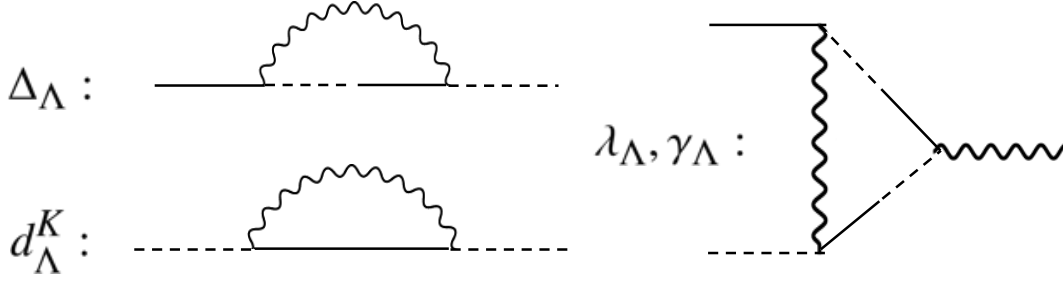
FIG. 5: One-loop contractions for Eq. (38). As for the flow of γ_Λ, the frequency derivative of the self-energy diagram for the retarded/advanced component (top left), generates the identical contraction as that for the noise vertex (right). This cancellation seems to be one reason for the generically scale-invariant nature of the rough phase as alluded to in the Introduction and observed in the numerics in Fig. 3.

C. One-loop flow equations

We now write down the explicit form of the flow equations following from expanding the master flow equation, Eq. (25), with the truncation specified above. For brevity, we will use an integration symbol that includes the cutoff derivatives:

$$\int = \int \frac{d^d \mathbf{k}}{(2\pi)^d} \int \frac{d\omega}{2\pi} \left[\dot{R}_\eta \partial_{R_\eta} + \dot{R}_\Lambda^R \partial_{R_\Lambda^R} + \dot{R}_\Lambda^A \partial_{R_\Lambda^A} \cdot \right] . \tag{37}$$

We get the expressions:

$$\partial_\Lambda (id_\Lambda^K) = \frac{-i}{2} \int \lambda_\Lambda^2 G_\Lambda^\eta(\omega) G_\Lambda^K(\omega, \mathbf{k})$$

$$\partial_\Lambda (-\Delta_\Lambda) = \frac{-i}{2} \int \lambda_\Lambda^2 G_\Lambda^\eta(\omega) \left(G_\Lambda^A(\omega, \mathbf{k}) + G_\Lambda^R(\omega, \mathbf{k}) \right)$$

$$\partial_\Lambda (-\lambda_\Lambda) = \frac{-i}{2} \int \lambda_\Lambda^3 G_\Lambda^\eta(\omega) \left(G_\Lambda^A(\omega, \mathbf{k})^2 + G_\Lambda^R(\omega, \mathbf{k})^2 \right) . \tag{38}$$

The corresponding Feynman contractions are shown in Fig. 5. At the one-loop level, there is no flow for the momentum renormalization factor $\partial_\Lambda A = 0$ and the flow of the frequency renormalization factor γ_Λ is obtained via the diagrammatic identity

$$\zeta_\gamma = -\frac{\Lambda}{\gamma_\Lambda} \partial_\Lambda \gamma_\Lambda = -\frac{\Lambda}{\lambda_\Lambda} \partial_\Lambda \lambda_\Lambda = \zeta_\lambda \tag{39}$$

also avoiding the necessity the perform frequency derivatives on the cutoff.

Severe diagrammatic redundancies appear in gauge theories (for example QED or the CP^N-model), there as a consequence of truly conserved global charges [42, 43]. Here, the cancellation

17

is probably a leftover effect of the expansion of the action in powers of $\tilde{\phi}\phi$, which can be traced back to a gauge transformation related to the Galilean invariance for temporally white noise [30].

In addition to the anomalous exponents in Eq. (39), we define the rescaled variables for the mass variable and the noise vertex

$$\tilde{\Delta} = \frac{\Delta_\Lambda}{\gamma_\Lambda \Lambda^2}$$

$$\tilde{\lambda} = \frac{\lambda_\Lambda}{\Lambda^{(4-d)/2} A_\Lambda^{d/4} \gamma_\Lambda^{1-d/4} \sqrt{\pi}} \tag{40}$$

and the slope of the statistical Keldysh component

$$\zeta_{d^K} = -\frac{\Lambda}{d_\Lambda^K} \partial_\Lambda d_\Lambda^K . \tag{41}$$

For completeness, we will write out the analogous exponent for the momentum factor $\zeta_A = -\frac{\Lambda}{A_\Lambda} \partial_\Lambda A_\Lambda$ in the equations below, but it vanishes at the one-loop level.

The various β-functions following from explicit evaluation of Eqs. (38) take on the simple form:

$$\Lambda \partial_\Lambda \tilde{\Delta} = \left(-2 + \zeta_\gamma\right) \tilde{\Delta} + \tilde{\lambda}^2 D_{\lambda^2}[\tilde{\Delta}] \tag{42}$$

$$\Lambda \partial_\Lambda \tilde{\lambda} = \left(\frac{d-4}{2} + \frac{d}{4}\zeta_A + (1 - \frac{d}{4})\zeta_\gamma - \zeta_\lambda\right) \tilde{\lambda}$$

together with the anomalous exponents

$$\zeta_A = 0$$

$$\zeta_{d^K} = \tilde{\lambda}^2 S_{\lambda^2}[\tilde{\Delta}]$$

$$\zeta_\gamma = \tilde{\lambda}^2 G_{\lambda^3}[\tilde{\Delta}] = \zeta_\lambda . \tag{43}$$

Invoking $\zeta_A = 0$ and the identity $\zeta_\gamma = \zeta_\lambda$ the flow equation for the noise vertex simplifies to

$$\Lambda \partial_\Lambda \tilde{\lambda} = \left(\frac{d-4}{2} - \frac{d}{4}\zeta_\gamma\right) \tilde{\lambda} . \tag{44}$$

Partial cancellations in β-functions can be a reason for the appearance of anomalous exponents that depend only on dimensionality [44] and sometimes critical phases rather than critical points.

The fixed point structure is determined by dimensionality d and the properties of the three threshold functions $D_{\lambda^2}[\tilde{\Delta}]$, $S_{\lambda^2}[\tilde{\Delta}]$, and $G_{\lambda^3}[\tilde{\Delta}]$, which depend on the mass variable $\tilde{\Delta}$ and dimensionality $d = 1, 2, 3$. The analytic expressions and various limiting cases for the threshold functions are given in Appendix A.

18

IV. SOLVING THE FLOW

In this section, we solve the flow equations (42,43) first analytically in two limit cases complementary to the numerical solutions exhibited in the key results section I B. The initial value for the mass variable is zero $\Delta_{\Lambda_0} = 0$, having in mind a gapless interface before turning on the coupling to the noise. We will vary strength of the noise vertex λ_Λ to tune through the phase diagram shown Sec. I B from the massive phase (small initial $\tilde{\lambda}_{\Lambda_0}$) to the rough, but gapless phase (large $\tilde{\lambda}_{\Lambda_0}$) via critical point to the rough phase at $\tilde{\lambda}_{\Lambda_0,c}$.

A. Hyperthermal fixed point in the rough phase

In $d < 4$, Eqs. (43,44) admit a stable non-Gaussian fixed point ($\Lambda\partial_\Lambda\tilde{\lambda} = 0$) solution

$$\zeta_\gamma = \frac{2(d-4)}{d}$$

$$\tilde{\lambda}_*^2 = \frac{2(d-4)}{d\,G_{\lambda^3}[\tilde{\Delta}_*]} \tag{45}$$

provided the equation for the mass ($\Lambda\partial_\Lambda\tilde{\Delta} = 0$) has a solution

$$\tilde{\Delta}_* = \frac{d-4}{4}\frac{D_{\lambda^2}[\tilde{\Delta}_*]}{G_{\lambda^3}[\tilde{\Delta}_*]} \tag{46}$$

such that $\tilde{\lambda}_*^2 > 0$ with $\tilde{\lambda}$ a real-valued number. This is indeed the case in $d = 1, 2, 3$ as is shown in Fig. 6 for $d = 2$. Of course, a fixed point $\tilde{\Delta}^*$ means that the physical mass vanishes during the flow

$$\Delta = \tilde{\Delta}^*\Lambda^2\gamma \underset{\Lambda\to 0}{\to} 0 \tag{47}$$

implying that the entire rough phase is gapless. This fixed point is accompanied by a set of critical exponents including the dynamical exponent

$$z = 2 + \zeta_A - \zeta_\gamma = 2 - \zeta_\gamma \tag{48}$$

collected in Table I. In the rough phase, the strong-coupling between the "flat $z = \infty$ spectrum" (local in space) of the noise propagator and the bare $z = 2$ overdamped ϕ-dynamics leads to z-values intermediating between the two values. Note that the steep flow when the scaling of the roughening transition changes to that of the rough phase in Fig. 2, is due to a change of sign of the threshold function for ζ_γ. This function, $G_{\lambda^3}[\tilde{\Delta}]$, is plotted in the Appendix A. Self-organized and generically scale-invariant phases in open systems have of course been discussed in a variety of contexts (see e.g. Hwa and Kardar [44] for a one-loop analysis of sandpile models and Ref. 45 for a broader discussion on symmetries).
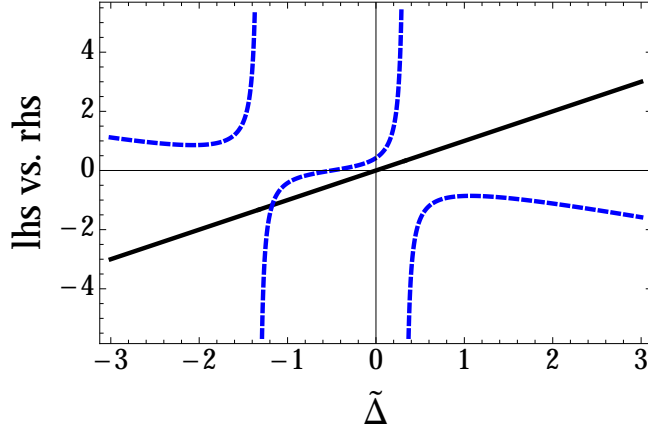
19

FIG. 6: Fixed point for $\tilde{\Delta}^* = -1.174$ in the rough phase in $d = 2$ from finding intersections of the left-hand-side of Eq. (46) (black line) with its right-hand-side (blue, dashed line). As at the Wilson-Fisher fixed point for the $O(n)$ model [46], the rough phase fixed point, $(\tilde{\Delta}^* = -1.396, \tilde{\lambda}^* = 10.154)$ also in $d = 3$, lies at negative mass in the plane of rescaled mass vs. rescaled coupling. This is true in all dimensions $d = 1, 2, 3$.

B. Fixed point at the roughening transition

The fixed point at the roughening transition (rt) is analyzed in changed variables

$$\tilde{\Delta}_{rt} = \tilde{\Delta}\Lambda^2\gamma^2$$
$$\tilde{\lambda}_{rt} = \tilde{\lambda}\Lambda^2\gamma^2 \tag{49}$$

which attain fixed points at the roughening transition, $(\tilde{\Delta}_{rt}^* = -5.81, \tilde{\lambda}_{rt}^* = 23.33)$ in $d = 3$, whose ratio turns out to be fixed to be $\left|\frac{\tilde{\lambda}_{rt}^*}{\tilde{\Delta}_{rt}^*}\right| = 3\pi\sqrt{\frac{2}{11}}$. This leads to an automatic fulfillment of the vanishing of the β-function indicative of an asymptotically unstable fixed point. In the numerics, this is reflected by shorter and somewhat more wobbly scaling plateaus of the mass and vertex when compared to the stable fixed point of the rough phase. This means that the physical mass vanishes $\Delta_\Lambda = \tilde{\Delta}_{rt}/\gamma \sim \Lambda^{\zeta_\gamma^{rt}}$ as can be seen in Fig. 7.

For the suitably rescaled noise vertex, we can write the flow equation

$$\partial_t\tilde{\lambda}_{rt} = \left(\frac{d}{2} - (1 + \frac{d}{4})\zeta_{\gamma_{rt}} - \zeta_{\lambda_{rt}}\right)\tilde{\lambda}_{rt}, \tag{50}$$

which implies Eq. (10) (with $\zeta_{\gamma_{rt}} = \zeta_{\lambda_{rt}}$). The emergent thermal fluctuation-dissipation relation is easily seen as follows. When $\tilde{\Delta}_{rt}^*$ attains a constant fixed point value, the "old" variable $\tilde{\Delta}$ must diverge. Expanding the threshold functions in Appendix A for the Keldysh component (in "old"

20

variables and for concreteness in $d = 3$)

$$\zeta_{d^K} = \tilde{\lambda}^2 S_{\tilde{\lambda}^2}[\tilde{\Delta}] \underset{\tilde{\Delta}\to\infty}{\to} \approx \tilde{\lambda}^2 \frac{1}{3\pi^2\tilde{\Delta}^2} = \tilde{\lambda}^2 G_{\lambda^3}[\tilde{\Delta} \to \infty] = \zeta_\gamma .\tag{51}$$

Note that the ratio $\frac{\tilde{\lambda}^2}{\tilde{\Delta}^2}$ is invariant under the variable change Eq. (49) and consequently $\zeta_\gamma^{\mathrm{rt}} = \zeta_{d^K}^{\mathrm{rt}}$ as seen in the explicit flows in Subsec. I B and Subsec. IV C.

C.   Numerical flows

We briefly describe the numerical procedure and initial conditions for the explicit flows in Subsec. I B. We also show a few of more plots: Fig. 7,8 for flows in the massive phase upon approaching the roughening transition and Fig. 9 as exemplary flow deep in the rough phase. The coupled flow equations (42,43) are integrated using a fourth order Runge Kutta routine (results did not change from using different routines) from high frequencies $\Lambda_0 = 10$ down to $\Lambda = 0$ using the momentum-integrated version of the threshold functions given in the Appendix A. We always
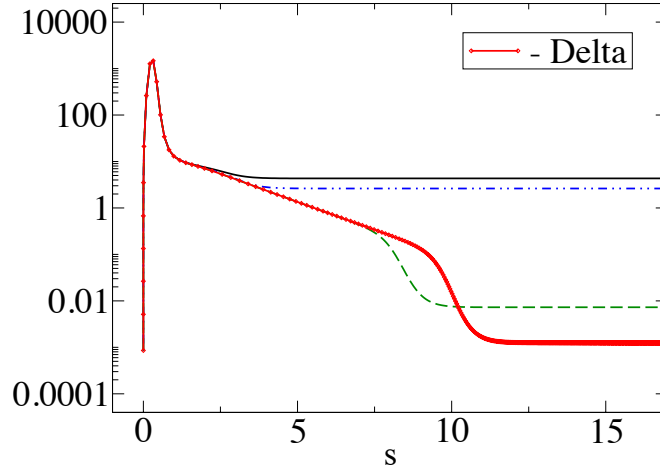

FIG. 7: Flow of the physical (non-rescaled) mass $-\Delta_\Lambda$ in $d = 3$ upon approaching the roughening transition from the massive phase for different values of the initial noise vertex in double logarithmic graph (with $s = -\log[\Lambda/\Lambda_0]$ the flow goes from the UV (left of plot) to IR (right of plot)). The mass is initially numerically zero $\Lambda_{s=0} = 0$. The red line is closest to the roughening transition $\tilde{\lambda}_{\Lambda_0,c}$ from below while the black line has a $\tilde{\lambda}_{\Lambda_0}$ furthest away from $\tilde{\lambda}_{\Lambda_0,c}$. For infinite numerical accuracy the power-law linear scaling with slope $\zeta_\gamma^{\mathrm{rt}} = 6/11 = 0.54$ from Eq. (10) for the roughening transition would extend longer and longer.
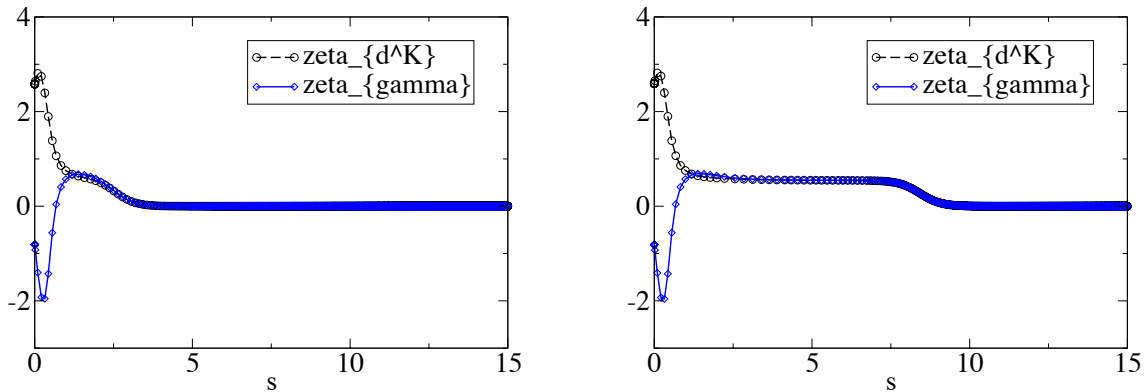
21

FIG. 8: Flow of the anomalous exponents when approaching the roughening transition from the massive phase. Left: $\tilde{\lambda}_{\Lambda_0} = 6.43$, Right: $\tilde{\lambda}_{\Lambda_0} = 6.442946808$. The closer the noise vertex is tuned to the critical value, the longer for the scaling plateau at which $\zeta_{d^K} = \zeta_\gamma = 0.54$ for $d = 3$ from Eq. (10). The flow goes from the UV (left of plot) to IR (right of plot) via $\Lambda = \Lambda_0 \exp(-s)$. At some point the scaling stops, both anomalous exponents become zero, because we are still in the massive phase.

begin the flow with zero initial mass $\Delta_{\Lambda_0} = \tilde{\Delta}_0$ as appropriate for the gapless interface. The initial value of the rescaled noise vertex $\tilde{\lambda}_{\Lambda_0}$ is varied to obtain the phase diagram Fig. 1. The condition for the phase boundary is the vanishing of the physical mass in the infrared $\Delta_{\Lambda \to 0} \to 0$.

V. CONCLUSIONS

This paper pursued the strategy to (i) take an important universality class for non-equilibrium statistical mechanics (Burgers-Kardar-Parisi-Zhang equation), (ii) strip it from an important conservation law(s) (Galilean invariance), and (iii) compute the phase diagram and critical exponents using the dynamic renormalization group.

We broke the Galilean invariance by accounting for temporal correlations in the random driving force. The chief consequence of this is the absence of a fluctuation-dissipation relation even in $d = 1$ for any noise level, and in $2 \leq d < 4$ for sufficiently strong noise levels. We penetrated this strong noise "rough or turbulent" phase within a dynamic RG flow using frequency rescaling techniques that took care of long-time correlations in the noise. We computed exponents to one-loop order, essentially controlled close to four space dimensions $d = 4$. We showed that the rough phase is an example of generic scale invariance in the sense that its emergent gaplessness does
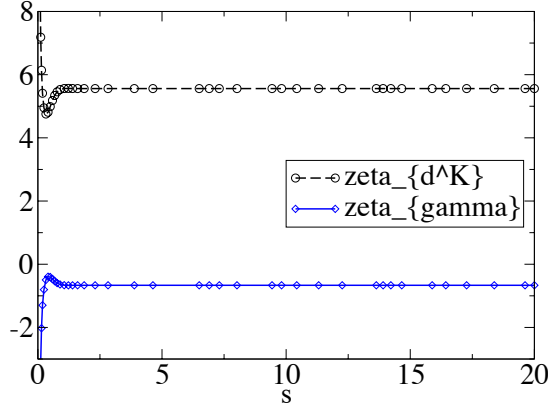
22

FIG. 9: Flows deep in the rough phase in which no remnant of the roughening transition (as in Fig. 2) is visible and the anomalous exponents very quickly attain their rough phase fixed point values $\zeta_{d^K} = 5.56$ and $\zeta_\gamma = -0.66$ from Table I in $d = 3$. Initial value of the noise vertex is $\tilde{\lambda}_{\Lambda_0} = 30 \gg \tilde{\lambda}_{\Lambda_0,c} = 6.4429468082319$. The flow goes from the UV (left of plot) to IR (right of plot) via $\Lambda = \Lambda_0 \exp(-s)$.

not require fine tuning and traced this back to explicit cancellations in the one-loop β-functions. Higher loop analysis and numerical simulations will be needed to determine the fate of our theory beyond one-loop.

Intriguing extensions of this work are quantum liquids and superfluids [47–49] (in which more exotic types of noise can potentially be applied [19, 20]), and waves in time-dependent random media [50, 51]. With regard to recent related works on nonlinear fluctuating hydrodynamics [52, 53], it will be interesting to systematically explore the role of broken conservation laws onto crossover time-scales in dynamics and transport [54].

Appendix A: Threshold functions

We here tabulate the threshold functions appearing in the flow equations (42,43), $D_{\lambda^2}[\tilde{\Delta}]$, $S_{\lambda^2}[\tilde{\Delta}]$, and $G_{\lambda^3}[\tilde{\Delta}]$. We will give the pre-momentum integrated expression for general dimension d and the post-momentum integrated expression only for $d = 2$; the other dimensions do not qualitatively change their form.

The flow of the Keldysh component is determined by

$$
S_{\lambda^2}^{(d)}[\tilde{\Delta}] = \int \frac{d^d\tilde{k}}{(2\pi)^d} \frac{2\left(\left(\tilde{\Delta} + \tilde{\mathbf{k}}^2\right)^2 + 3\right)}{\left(\left(\tilde{\Delta} + \tilde{\mathbf{k}}^2\right)^2 + 1\right)^2}\Bigg|_{0 \leq \tilde{\mathbf{k}}^2 \leq 1}
$$

$$
\stackrel{d=2}{=} \frac{-2\left(\tilde{\Delta}^2 + 1\right)(\tilde{\Delta}(\tilde{\Delta} + 2) + 2)\tan^{-1}(\tilde{\Delta}) + 2\left(\tilde{\Delta}^2 + 1\right)(\tilde{\Delta}(\tilde{\Delta} + 2) + 2)\tan^{-1}(\tilde{\Delta} + 1) - \tilde{\Delta}(\tilde{\Delta} + 1) + 1}{2\pi\left(\tilde{\Delta}^2 + 1\right)(\tilde{\Delta}(\tilde{\Delta} + 2) + 2)} .
$$

$$(A1)$$

The flow of the mass variable is determined by

$$
D_{\lambda^2}^{(d)}[\tilde{\Delta}] = \int \frac{d^d\tilde{k}}{(2\pi)^d} \frac{2\left(\tilde{\Delta} + \tilde{\mathbf{k}}^2\right)\left(\left(\tilde{\Delta} + \tilde{\mathbf{k}}^2\right)^2 + 3\right)}{\left(\left(\tilde{\Delta} + \tilde{\mathbf{k}}^2\right)^2 + 1\right)^2}\Bigg|_{0 \leq \tilde{\mathbf{k}}^2 \leq 1}
$$

$$
\stackrel{d=2}{=} \frac{\frac{4\tilde{\Delta}+2}{(\tilde{\Delta}^2+1)(\tilde{\Delta}(\tilde{\Delta}+2)+2)} + \log\left(\frac{2\tilde{\Delta}+1}{\tilde{\Delta}^2+1} + 1\right)}{4\pi} .
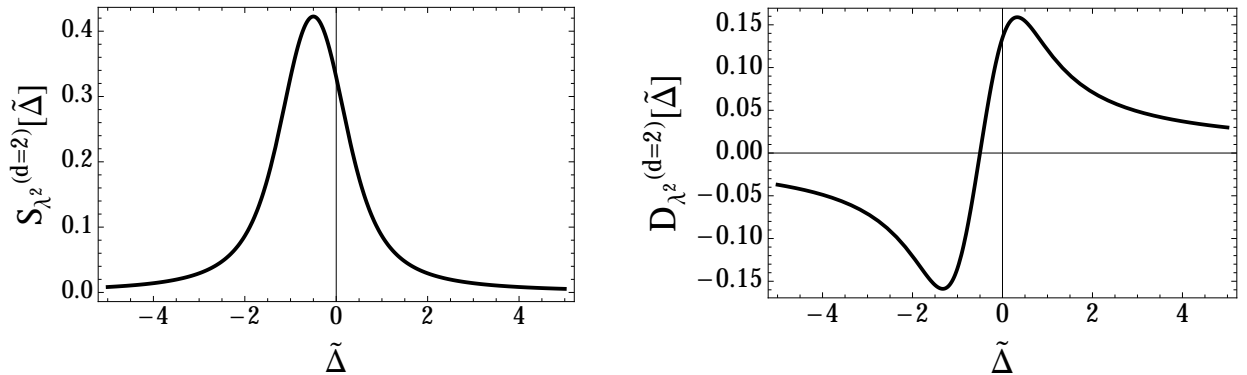$$

$$(A2)$$

FIG. 10: Plots of the threshold functions for the Keldysh component (left) and the mass (right) in $d = 2$.
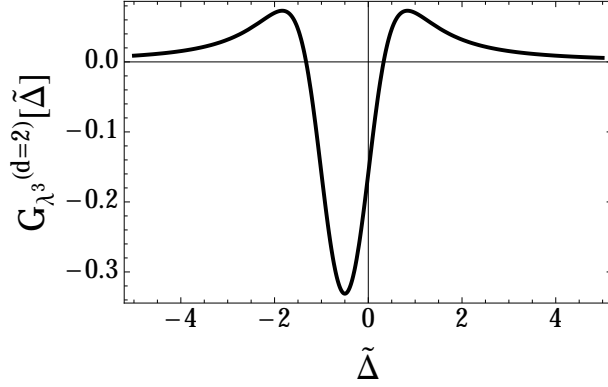
FIG. 11: Plot of the threshold functions for the noise vertex/frequency renormalization factor in $d = 2$.

The flow of the noise vertex (and the frequency renormalization factor) is determined by

$$G_{\lambda^3}^{(d)}[\tilde{\Delta}] = \int \frac{d^d \tilde{k}}{(2\pi)^d} \left. \frac{2\left(\left(\tilde{\Delta} + \tilde{\mathbf{k}}^2\right)^2 \left(\left(\tilde{\Delta} + \tilde{\mathbf{k}}^2\right)^2 + 6\right) - 3\right)}{\left(\left(\tilde{\Delta} + \tilde{\mathbf{k}}^2\right)^2 + 1\right)^3} \right|_{0 \le \tilde{k}^2 \le 1}$$

$$\stackrel{d=2}{=} \frac{\tilde{\Delta}(\tilde{\Delta} + 1)\left(\tilde{\Delta}^2 + \tilde{\Delta} + 1\right)\left(\tilde{\Delta}^2 + \tilde{\Delta} + 6\right) - 4}{2\pi \left(\tilde{\Delta}^2 + 1\right)^2 (\tilde{\Delta}(\tilde{\Delta} + 2) + 2)^2} \, . \tag{A3}$$

[1] H. M. Jaeger, and A. J. Liu, *Far-From-Equilibrium Physics: An Overview*, arXiv:1009.4874, Condensed Matter and Materials Physics: the science of the world around us, National Academies Press, Washington, DC (2007).

[2] S. Sotiriadis, and J. Cardy, *Quantum quench in interacting field theory: A self-consistent approximation*, Phys. Rev. B **81**, 134305 (2010).

[3] K. A. Takeuchi, and M. Sano, *Universal Fluctuations of Growing Interfaces: Evidence in Turbulent Liquid Crystals*, Phys. Rev. Lett. **104**, 230601 (2010).

[4] P. J. Yunker, M. A. Lohr, T. Still, A. Borodin, D. J. Durian, and A. G. Yodh, *Effects of Particle Shape on Growth Dynamics at Edges of Evaporating Drops of Colloidal Suspensions*, Phys. Rev. Lett. **110**, 035501 (2013).

[5] M. Kardar, G. Parisi, and Y.-C. Zhang, *Dynamic Scaling of Growing Interfaces*, Phys. Rev. Lett. **56**, 889 (1986).

[6] D. Forster, D. R. Nelson, and M. J. Stephen, *Large-distance and long-time properties of a randomly stirred fluid*, Phys. Rev. A **16**, 732 (1977).

[7] M. Kardar, *Replica Bethe Ansatz Studies of Two-Dimensional Interfaces with Quenched Random Impurities*, Nucl. Phys. B **290**, 582 (1987).

[8] E. Brunet and B. Derrida, *Probability distribution of the free energy of a directed polymer in a random medium*, Phys. Rev. E **61**, 6789 (2000).

[9] P. Calabrese and P. Le Doussal, *Exact Solution of the Sardar-Parisi-Zhang equation with Flat Initial Conditions*, Phys. Rev. Lett. **106**, 250603 (2011).

[10] P. Calabrese, M. Kormos and P. Le Doussal, *From the sine-Gordon field theory to the Sardar-Parisi Zhang growth equation*, arXiv:1405.2582 (2014).

[11] G. Grinstein, M. A. Munoz, and Y. Tu, *Phase Structure of Systems with Multiplicative Noise*, Phys. Rev. Lett. **76**, 4376 (1996).

[12] E. Medina, T. Hwa, M. Kardar, Y.-C. Zhang, *Burgers equation with correlated noise: Renormalization-group analysis and applications to directed polymers and interface growth*, Phys. Rev. A **39**, 3053 (1989).

[13] P. Bak, C. Tang, and K. Wiesenfeld, *Self-Organized Criticality: An Explanation of $1/f$ Noise*, Phys. Rev. Lett. **59**, 381 (1987).

[14] C.-H. Lam, L. M. Sander, and D. E. Wolf, *Surface growth with temporally correlated noise*, Phys. Rev. A **46**, R6128 (1992).

[15] T. Halpin-Healy and Y.-C. Zhang, *Kinetic roughening phenomena, stochastic growth, directed polymers and all that. Aspects of multidisciplinary statistical mechanics*, Physics Reports **254**, 215 (1995).

[16] E. Katzav and M. Schwartz, *Kardar-Parisi-Zhang equation with temporally correlated noise: A self-consistent approach*, Phys. Rev. E **70**, 011601 (2004).

[17] J. Bonart, L. F. Cugliandolo, and A. Gambassi, *Critical Langevin dynamics of the $O(N)$-Ginzburg-Landau model with correlated noise*, J. Stat. Mech. P01014 (2012).

[18] E. G. Dalla Torre, E. Demler, T. Giamarchi, and E. Altman, *Quantum critical states and phase transitions in the presence of non-equilibrium noise*, Nat. Phys. **6**, 806 (2010).

[19] E. G. Dalla Torre, E. Demler, T. Giamarchi, and E. Altman, *Dynamics and universality in noise-driven dissipative systems*, Phys. Rev. B **85**, 184302 (2012).

[20] M. Buchhold, and S. Diehl, *Non-Equilibrium Universality in the Heating Dynamics of Interacting Luttinger Liquids*, arXiv:1404.3740 (2014).

[21] T. Nattermann, and L.-H Tang, *Kinetic surface roughening. I. The Kardar-Parisi-Zhang equation in the weak-coupling regime*, Phys. Rev. A **45**, 715 (1992).

[22] E. Frey, and U. C. Täuber, *Two-loop renormalization-group analysis of the Burgers-Kardar-Parisi-Zhang equation*, Phys. Rev E. **50**, 1024 (1994).

[23] J. Berges, K. Boguslavski, S. Schlichting, and R. Venugopalan, *Basin of attraction for turbulent thermalization and the range of validity of classical-statistical simulations*, arXiv:1312.5216 (2013).

[24] S. Mathey, T. Gasenzer, and J. M. Pawlowski, *Anomalous scaling at non-thermal fixed points of Burgers' and Gross-Pitaevskii turbulence*, arXiv:1405.7652 (2014).

[25] G. Grinstein, *Generic scale invariance in classical non equilibrium systems*, Journal of Applied Physics **69**, 5441 (1991).

[26] G. Grinstein and D.-H. Lee, *Generic Scale Invariance and Roughening in Noisy Model Sandpiles and Other Driven Interfaces*, Phys. Rev. Lett. **66**, 177 (1991).

[27] J. P. Bouchaud, M. Mezard, and G. Parisi, *Scaling and intermittency in Burgers turbulence*, Phys. Rev. E **52**, 3656 (1995).

[28] A. Kamenev, *Field Theory of Non-Equilibrium Systems*, Cambridge University Press, Cambridge (2011).

[29] E. G. Dalla Torre, S. Diehl, M. D. Lukin, S. Sachdev, and P. Strack, *Keldysh approach for nonequilibrium phase transitions in quantum optics: Beyond the Dicke model in optical cavities*, Phys. Rev. A **87**, 023831 (2013).

[30] H. K. Janssen, U. C. Täuber, and E. Frey, *Exact results for the Kardar-Parisi-Zhang equation with spatially correlated noise*, Eur. Phys. J B **9**, 491 (1999).

[31] D. A. Huse, C. L. Henley, and D. S. Fisher, *Huse, Henley, and Fisher Respond*, Phys. Rev. Lett. **55**, 2924 (1985).

[32] U. Deker and F. Haake, *Fluctuation-dissipation theorems for classical processes*, Phys. Rev. A **11**, 2043 (1975).

[33] R. Gezzi, T. Pruschke, and V. Meden, *Functional renormalization group for nonequilibrium quantum many-body systems*, Phys. Rev. B **75**, 045324 (2007).

[34] L. M. Sieberer, S. D. Huber, E. Altman, and S. Diehl, *Non-equilibrium Functional Renormalization for Driven-Dissipative Bose-Einstein Condensation*, Phys. Rev. B **89**, 134310 (2014).

[35] L. Canet, H. Chaté, B. Delamotte, and N. Wschebor, *Nonperturbative Renormalization Group for the Kardar-Parisi-Zhang Equation*, Phys. Rev. Lett. **104**, 150601 (2010).

27

[36] T. Kloss, L. Canet, and N. Wschebor, *Nonperturbative renormalization group for the stationary Kardar-Parisi-Zhang equation: Scaling functions and amplitude rations in 1+1, 2+1, and 3+1 dimensions*, Phys. Rev. E **86**, 051124 (2012).

[37] T. Kloss, L. Canet and N. Wschebor, *Strong coupling phases of the anisotropic Kardar-Parisi-Zhang equation* arXiv:1409.8314 (2014).

[38] T. Kloss, L. Canet, B. Delamotte, and N. Wschebor, *Kardar-Parisi-Zhang equation with spatially correlated noise: A unified picture from nonperturbative renormalization group*, Phys. Rev. E **89**, 022108 (2014).

[39] P. Strack, R. Gersch, and W. Metzner, *Renormalization group flows for fermionic superfluids at zero temperature*, Phys. Rev. B **78**, 014522 (2008).

[40] K.-U. Giering, and M. Salmhofer, *Self-energy flows in the two-dimensional repulsive Hubbard model*, Phys. Rev. B **86**, 245122 (2012).

[41] W. Metzner, M. Salmhofer, C. Honerkamp, V. Meden, and K. Schoenhammer, *Functional renormalization group approach to correlated fermion systems*, Rev. Mod Phys. **84**, 299 (2012).

[42] A. M. Polyakov, *Gauge fields and Strings*, CRC Press (Chur) (1987).

[43] Y. Huh, P. Strack, and S. Sachdev, *Conserved current correlators of conformal field theories, in* $2 + 1$ *dimensions*, Phys. Rev. B **88**, 155109 (2013).

[44] T. Hwa, and M. Kardar, *Dissipative Transport in Open Systems: An Investigation of Self-Organized Criticality*, Phys. Rev. Lett. **62**, 1813 (1989).

[45] G. Grinstein, D.-H. Lee, and S. Sachdev, *Conservation laws, Anisotropy, and "Self-Organized Criticality" in Noisy Nonequilibrium Systems*, Phys. Rev. Lett. **64**, 1927 (1990).

[46] K. G. Wilson and M. E. Fisher, *Critical Exponents in 3.99 Dimensions*, Phys. Rev. Lett. **28**, 240 (1971).

[47] M. Kulkarni, and A. Lamacraft, *Finite-temperature dynamical structure factor of the one-dimensional Bose gas: From the Gross-Pitaevskii to the Kardar-Parisi-Zhang universality class of dynamical critical phenomena*, Phys. Rev. A **88**, 021603 (R) (2013).

[48] M. Arzamasovs, F. Bovo, and D. M. Gangardt, *Kinetics of Mobile Impurities and Correlation Functions in One-Dimensional Superfluids at Finite Temperature*, Phys. Rev. Lett. **112**, 170602 (2014).

[49] E. Altman, *et al.*, *Two-dimensional superfluidity of exciton-polaritons requires strong anisotropy*, arXiv:1311.0876 (2013).

[50] L. Levi, Y. Krivolapov, S. Fishman, and M. Segev, *Hyper-transport of light and stochastic acceleration*

by evolving disorder, Nature Physics **8**, 912 (2012).

[51] L. Saul, M. Kardar, and N. Read, *Directed waves in random media*, Phys. Rev. A **45**, 8859 (1992).

[52] H. v. Beijeren, *Exact Results of Anomalous Transport in One-Dimensional Hamiltonian Systems*, Phys. Rev. Lett. **108**, 180601 (2012).

[53] C. B. Mendl, and H. Spohn, *Dynamic Correlators of Fermi-Pasta-Ulam Chains and Nonlinear Fluctuating Hydrodynamics*, Phys. Rev. Lett. **111**, 230601 (2013).

[54] J. Lux, J. Müller, A. Mitra, and A. Rosch, *Hydrodynamic long-time tails after a quantum quench*, Phys. Rev. A **89**, 053608 (2014).

[55] The main motivation for using Keldysh is to lay a basis for generalizing our work to quantum systems. There, one expects the short time, short distance behavior still be dominated by quantum effects and then the KPZ scaling to emerge in the IR at long times and large distances (see e.g.: Refs. 47, 48). To capture also the crossover scales, one needs to use Keldysh.

[56] Even if "analytic" contributions do occur in the flow, one just has to carefully remove them by hand, checking first if the loop integrations are finite without any cutoff.

[57] For example, we tried momentum cutoffs of the form $R_\Lambda^\phi(\mathbf{k}) = -A(\Lambda^2 - \mathbf{k}^2)\theta(\Lambda^2 - \mathbf{k}^2)$ and for the noise propagator $R_\Lambda^\eta = \Lambda^2$ as well as $R_\Lambda^\eta(\mathbf{k}) = \Lambda^2\theta(\Lambda^2 - \mathbf{k}^2)$. The last choice "entangles" frequency of the noise with momenta of the ϕ-field, but the flow was qualitatively similar to the ones with the frequency cutoff. We believe the using a frequency cutoff is cleaner and the ability to do so a particular strength of the 1-PI functional flow equation (25).